

PIT Project Research Report: MD3
BS/TEST1 ABAQUS model using FEAST with shell elements

Martin Gillie
June 2000

The University of Edinburgh
School of Civil and Environmental Engineering
Crew Building
King's Buildings
West Mains Road
University of Edinburgh
EH9 3JN

Contents

1	Introduction	3
2	The Model of Test One	3
3	The Experimental Load Case	4
A	ABAQUS input for FEAST model of test 1	15
B	FEAI input file for the slab parallel to the ribs	25
C	FEAI input file for the slab perpendicular to the ribs	26

Abstract

This report describes the analysis of Cardington test 1 using the FEAST³ suite of programs. The finite element model used to represent the test is carefully described and the assumptions made in producing the model explained and justified. Consideration is then given to ensuring that realistic values are assigned to the various parameters in the numerical model for which it was not possible to obtain accurate values from the test data. A comparison of the predicted deflections of the model with the experimental deflections is made for the best data set. This comparison shows an excellent match.

1 Introduction

Modelling of the various tests carried out on the Cardington frame was undertaken using a number of approaches. This report describes the model developed to model the first of the Cardington tests using the FEAST suite of programs. It should be read in conjunction with report AM3,² which analyses the test based on the results of this model. The FEAST suite is described in report SS2.³

2 The Model of Test One

The layout of a typical floor of the Cardington frame showing the position of each of the tests is shown in Fig. 1. It can be seen that for test 1 there was a considerable area of cold structure separating the heated compartment from the edge of the building on all sides. This cold area remained very stiff in comparison to the heated compartment and so the compartment was well restrained laterally. As a result, it was not necessary to model the entire floor for a realistic finite element mesh to be developed because the lateral restraint could be accurately represented by rigid horizontal boundary conditions. A side effect of assuming rigid horizontal boundary conditions was to make it possible to use assume symmetry along a line perpendicular to the tested beam at mid-span. This approach resulted in the area of slab modelled for test one extending from the middle of the heated compartment to the column in the direction of the heated beam and to mid-span in each of the unheated bays adjacent to the heated compartment. This is shown in schematic form in Fig. 2 and the finite element mesh is shown in Figs. 3 to 5. Eight noded, reduced integration, 3-dimensional shell elements were used in a 30×30 regular grid. At each of the boundaries vertical displacement and rotation about an axis parallel to the line of the boundary were allowed while all other degrees of freedom were fixed. This arrangement produced a symmetry condition at all edges of the slab. The behaviour of the slab was governed by the FEAI program, as described in report SS2.³ This meant that all the important aspects of the slab's behaviour were modelled including material non-linearity, orthotropic, thermal expansion, non-linear thermal gradients and thermal curvature.

The beams and column were modelled as I-section, 2-noded linear beam elements. This meant that the local buckling that was seen to take place in the Cardington experiment would not be captured in the model. However it was shown in report MD4⁶ that this local behaviour did not effect the overall predictions of numerical models. By using beam elements rather than shell elements considerable computational time and resources were saved. As with the slab, where the beam elements coincided with the edge of the mesh, symmetry boundary conditions were used. The column was modelled from one floor below the floor on which the test took place to one floor above it, also with 2-noded linear beam elements. The bottom end of the column was fully fixed whilst at the top only vertical deflections were permitted. The behaviour of the steel in the beams and columns was that defined in Eurocode 3¹ and is shown in Fig. 6.

In the experiment the beam to beam and column to column connections were half-depth end plates.⁵ Such connections can be assumed to have little or no moment capacity; pinned connections were used in the finite element model to represent this condition. The slab was connected to the beams by shear studs that provided a very high degree of restraint and so rigid connections were specified numerically.

There were two kinds of load applied during the Cardington experiment; a static load and a thermal load. The total static load was 5.48 kN/m^2 and this was straight forward to apply numerically. The thermal loading was less clearly defined. The slab reference surface temperature-time curve was derived from the same set of sensors from which the vertical temperature profiles through the slab were obtained (report SS2³). The complete set of curves for this set of sensors is shown in Fig. 7. The temperature regime obtained from these sensors was applied over the whole of the heated area. For the calculation of thermal curvatures, thermal gradients were assumed to be linear through the depth of the slab and to increase linearly with time from zero to a final value during the course of the heating. As explained in report SS2³ this assumption of a linear gradient through the slab for calculating thermal curvatures is in contrast to the polynomial temperature profiles used for calculating the slab's material properties and stiffness. Experimental values of temperature-time relationships for the heated beam were taken from a set of sensors at mid-span and are shown in Fig. 8. Because of restrictions imposed by ABAQUS, it was not possible to allow for different forms of temperature-time curve for say the web and flanges of the beam. It was, however, possible for a linear temperature gradient to be specified over the depth of the beam. The form of the temperature-time curve applied numerically was that produced by the sensor on the web and the thermal gradient was given a value that resulted in the top and bottom flanges of the beam having their experimental temperatures at the end of the heating. The curves in Fig. 8 show that the temperature of the steel in the beam dropped slightly when there was a phase change at 820C. This drop was smoothed to a plateau for the numerical analysis.

The loading was applied in two stages. First the static load was applied whilst the structure unheated. The structure was then heated according to the temperature-time curves described above with the static load remaining unaltered. Geometric non-linearity was accounted for in the entire mesh for all of the analyses. To aid numerical convergence it was sometimes found advantageous to use the damping option available in ABAQUS.⁴ This option provided the model with an artificial mass matrix, and was particularly effective in preventing numerical instabilities resulting from local buckling in parts of the structure. The amount of damping that was applied could be varied and whenever this option was used, care was taken to ensure that the damping did not perturb the solution significantly.

The ABAQUS input file used for test 1 is shown in Appendix A together with the input files associated with FEAL.

3 The Experimental Load Case

The first problem in analysing the experimental load case was to determine suitable values for the parameters that defined it. Many of the details of the Cardington tests were well documented and so reproducing them in numerical models was straightforward. However, other information about the tests was poorly recorded or unavailable. In these areas it was necessary to make careful assumptions about the model input data and to establish to what extent the model was sensitive to these assumptions.

If the numerical models were to reveal the changing patterns of load transfer in the structure during the fire, they had to include adequate representation of all the physical phenomena present. A demonstration that a model matched the observed deflection pattern was not in itself sufficient to demonstrate that the model was accurately modelling the test. For this to be demonstrated the model also had to identify the key events during the fire, reveal the structural phenomena responsible for them and justify the conclusions using the fundamental principles of structural mechanics. However, for the purposes of establishing which of several sets of input data are the most representative of the Cardington test, it will be assumed that data sets that predict deflections that close to the observed deflections are more representative data sets than those that predict deflections that are less close. It is demonstrated in report AM3² that the data set chosen does indeed capture all the key structural phenomena. The parametric runs used a base set of parameters that, in the light of the available information, seemed the most logical and accurate before any analysis took place. These parameters were varied one at a time to determine the effect they had on the model.

The most significant of the assumptions that had to be made was the amount of thermal expansion in the slab. It will be shown in report AM3² that forces and deflections in the test are overwhelmingly dominated by the thermal expansion of the slab, that is, by the product αT for concrete. The exact value of α and both the spatial and temporal variation of T in the concrete were poorly known. Three runs were done with various values of αT and the results are shown in Fig. 9. The purpose of these runs was to determine the direct effect of thermal expansion on the analyses. Although the amount of thermal expansion was governed by both α and T , it was important to remember that varying T would have the side effect of altering the material properties in the section and that this in turn could alter the predicted deflections. To ensure that this side effect did not influence the results the peak value of T was held constant during the runs shown in Fig. 9 while the value of α was varied. The three values of α used were $0.85 \times 10^{-5} C^{-1}$, $0.95 \times 10^{-5} C^{-1}$ and $1.05 \times 10^{-5} C^{-1}$. In the middle of the temperature range these three runs can all be seen to produce predicted temperature-deflection curves that approximate to the experimental curve well. The closest match occurs with a coefficient of thermal expansion of $0.95 \times 10^{-5} C^{-1}$.

Another important variable for which a suitable value had to be established was the tensile strength of the concrete. The need for determining the value arose because of limitations in ABAQUS rather than from limitations in the test data. Because ABAQUS has to use a Newton-Raphson type solver⁴ when solving problems with combined static and thermal loading, it has severe difficulty in tracking the behaviour of structures that have negative stiffnesses. This meant that when using FEAI it was necessary to remove the descending branch of the material data curves³ and to assume ductile behaviour beyond the peak stress. The concrete compressive behaviour that results from this modification is shown in Fig. 10 - a small amount of stiffening was included to aid numerical convergence. The tensile strength of concrete is around one tenth of its compressive strength but only at very low strains. When a material model that does not allow for a descending branch of the stress-strain curve is used to represent concrete, it is necessary to decide whether the tensile strength at low strains or at high strains is to be modelled accurately. If it is decided to model the tensile strength at low strains accurately then it is necessary to allow the concrete to continue to carry stresses at higher strains - this can be viewed as having a poor representation of concrete cracking. Conversely, if the cracking of the concrete is to be modelled well then the initial tensile strength can no longer be included in the model. Both assumptions result in incorrect material behaviour for certain strain and curvature states. Comparisons of three behaviours for the tensile strength of concrete are shown in Fig. 11. The influence of changing the tensile behaviour of the concrete is most clearly seen at low temperatures. The initial deflection rate is strongly influenced by reducing the tensile capacity. At higher temperatures the form of the deflection curve is not strongly affected by the changes in the tensile behaviour. The reason for this is that at higher temperatures the slab is largely in compression as a result of restrained thermal expansion and so the tensile behaviour of the concrete has less significance.

The value of the thermal gradient to be used in the slab for calculating the thermal curvature was also unclear. The problem arose because it was necessary to specify a linear gradient numerically whereas in reality the gradient was highly non-linear, particularly at the end of the test. The problem is shown graphically in the Fig. 12. The results from using three different values of gradient are given in Fig. 13. From these curves it is clear that a linear gradient of $5C/mm$ produced a deflection curve that was close to parallel to the experimental curve for most of the temperature range.

Determining the form of the temperature-time curve to be used in heating the slab was not straight forward. The experimental data from the various sensors that was shown in Fig. 7, indicates that in reality the form of the temperature-time curve varied through the depth of the slab. Numerically only one curve could be specified and so a suitable approximation had to be arrived at. The temperature-time curve applied in the preceding parametric runs was that from the sensor 70mm below the top surface of the slab because this sensor was the closest to the slab reference surface. It is clear from the results of all the parametric runs that there is a discrepancy between the forms of the experimental deflection curve and the numerical deflection curves for slab temperatures above around 130C. Also, at this temperature, the the temperature-time curve that was input shows a different trend to the temperature-time curves produced by the other sensors, (Fig. 7). Because of this the model was run with a composite temperature-time curve. This curve used the data from the sensor 70mm below the top surface of the slab until a temperature of 130C was reached and the data from 40mm below the

top surface for higher temperatures. This run used what had been determined to be the optimum values for the various parameters considered in the parametric runs ($\alpha = 0.95 \times 10^{-5}$, concrete tensile strength equal to 1% of the compressive strength and a thermal gradient of 5C/mm). The results, shown in Figs. 14 and 15, demonstrate the model matched the experimental deflections very closely.

References

- [1] ENV. *Eurocode 3, Design of composite steel and concrete structures*, 1994.
- [2] M. Gillie. PIT Project Research Report AM3: Analysis of results from BS/TEST1 models, Part C FEAST shell models. Technical report, University of Edinburgh, 2000.
- [3] M. Gillie. PIT Project Research Report SS2: Development of generalised stress strain relationships for the concrete slab in shell models. Technical report, University of Edinburgh, 2000.
- [4] Hibbet, Karlson and Sorenson, Providence, Rhode Island, USA. *ABAQUS Users' Manual, Vols I to III, Ver 5.8*, 1998.
- [5] B.R. Kirby. The Behaviour of a Multi-storey Steel Framed Building Subjected to Fire Attack, Experimental Data. Technical report, British Steel, 1998.
- [6] M. O'Connor. PIT Project Research Report MD4: BS/Test1 ABAQUS model using shell elements for the beam and beam general section for the slab. Technical report, British Steel, 2000.

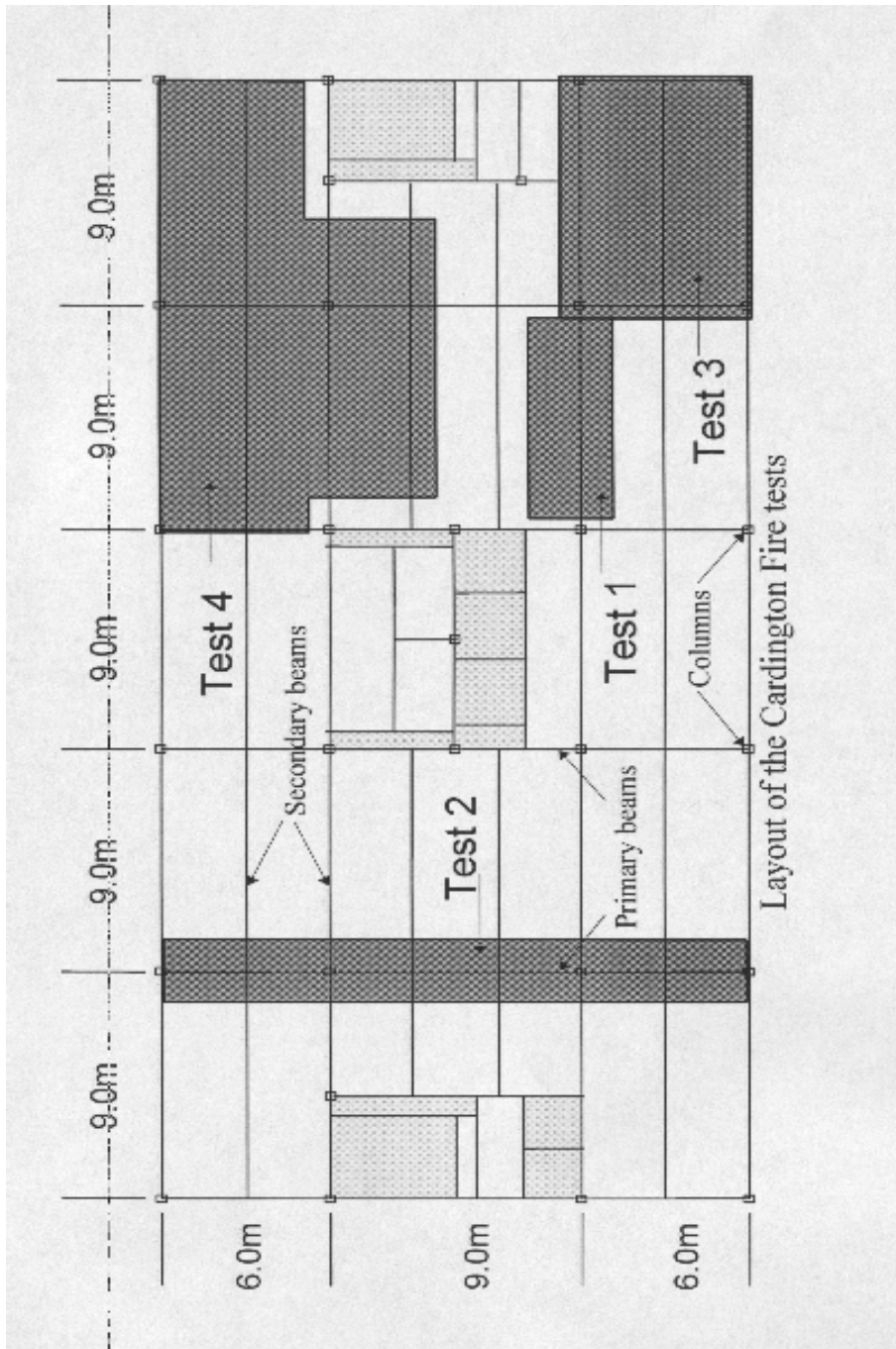


Figure 1: Layout of a typical floor of the Cardington frame showing the locations of the various tests. It should be noted that each test was carried out on a separate floor.

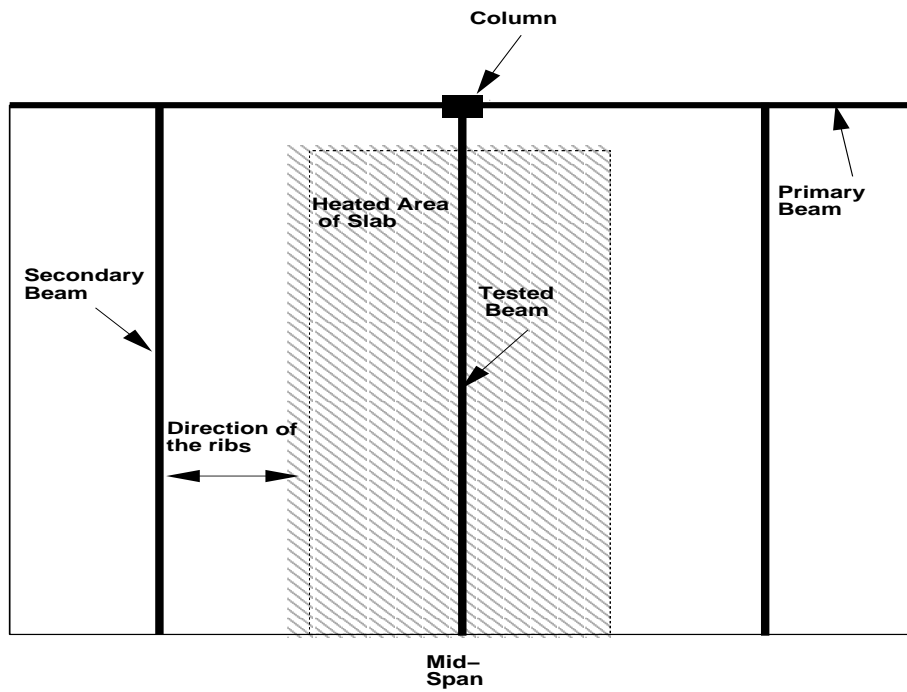


Figure 2: Schematic plan view of the area of the Cardington frame modelled for the analysis of test 1.

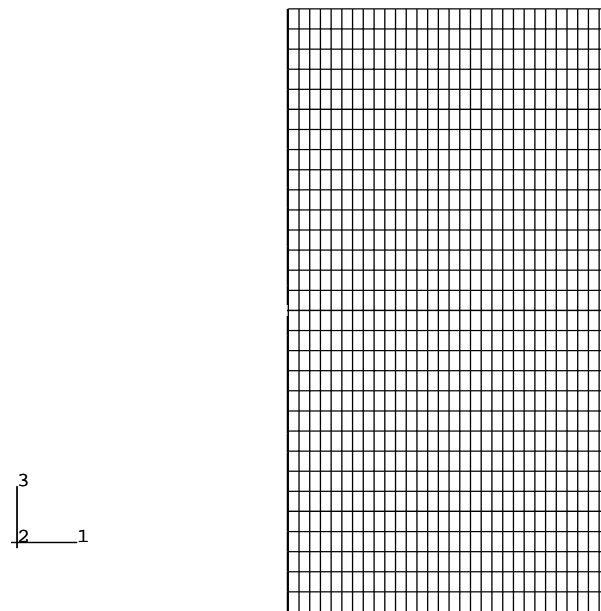


Figure 3: Plan view of the mesh used for modelling test 1 with shell elements.

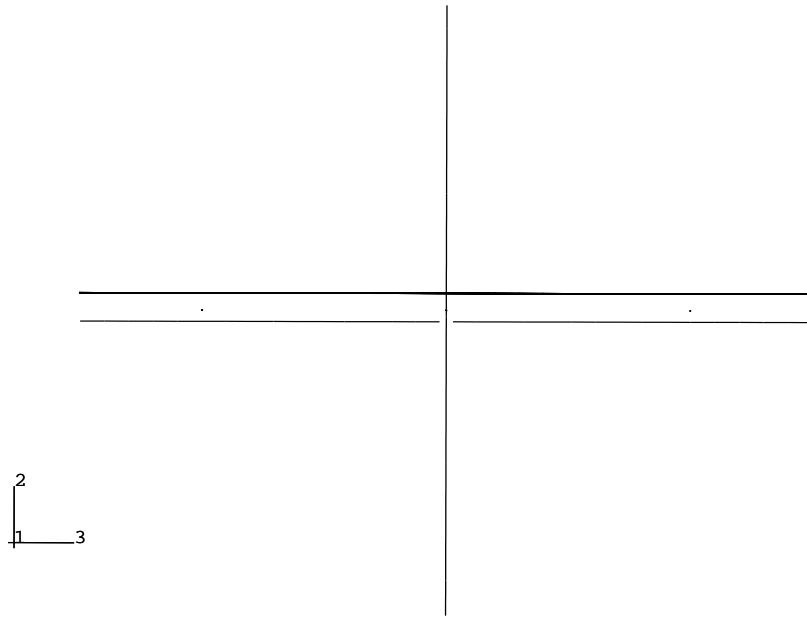


Figure 4: View of the mesh used for modelling test 1 with shell elements (axis of the tested beam runs into the paper).

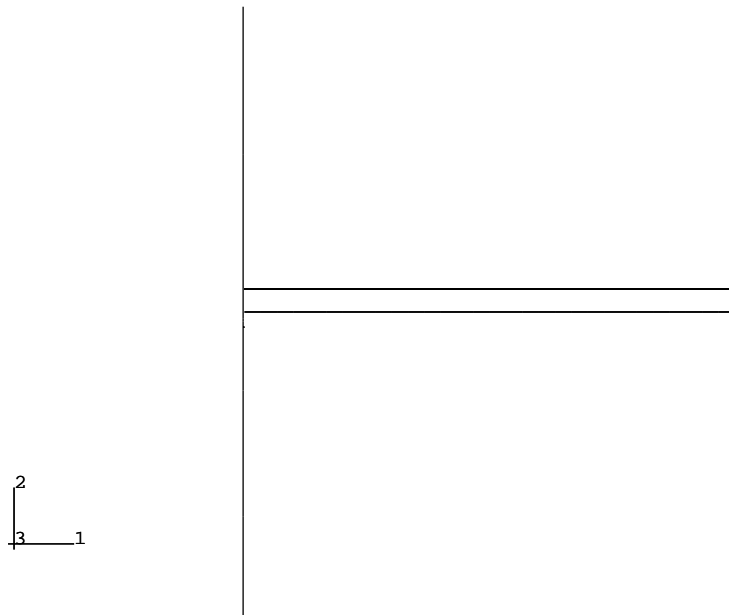


Figure 5: View of the mesh used for modelling test 1 with shell elements (axis of the tested beam runs left to right).

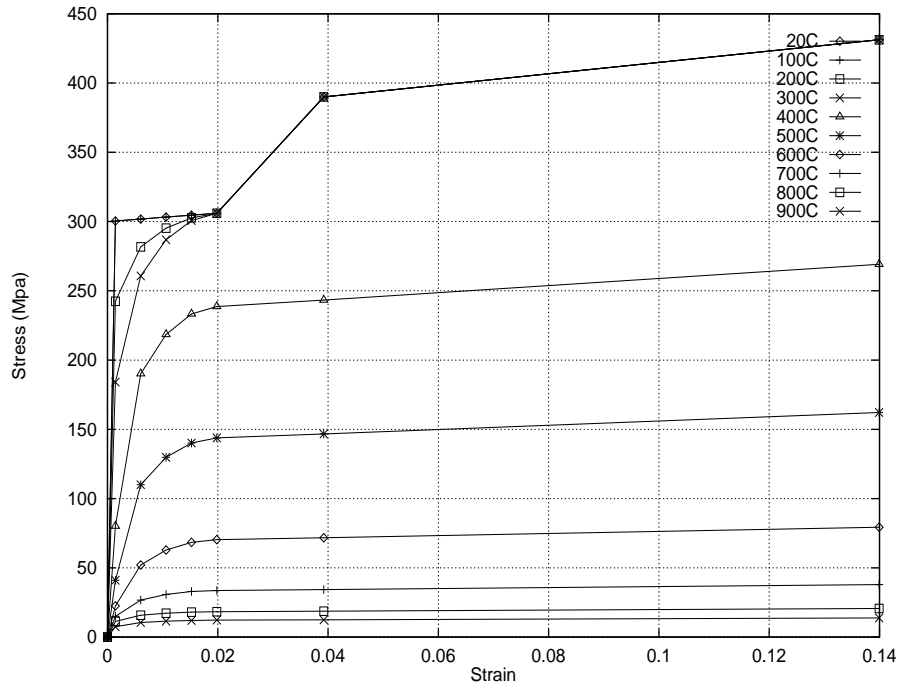


Figure 6: The steel material behaviour used for modelling Cardington test 1.

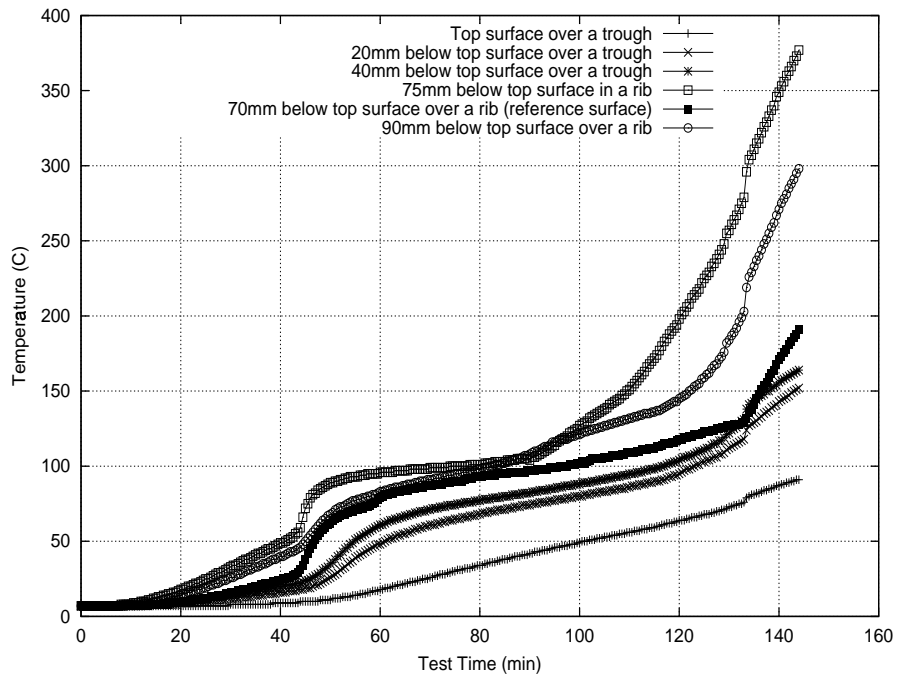


Figure 7: Experimental values of the slab temperature at various locations through its depth at a typical section.

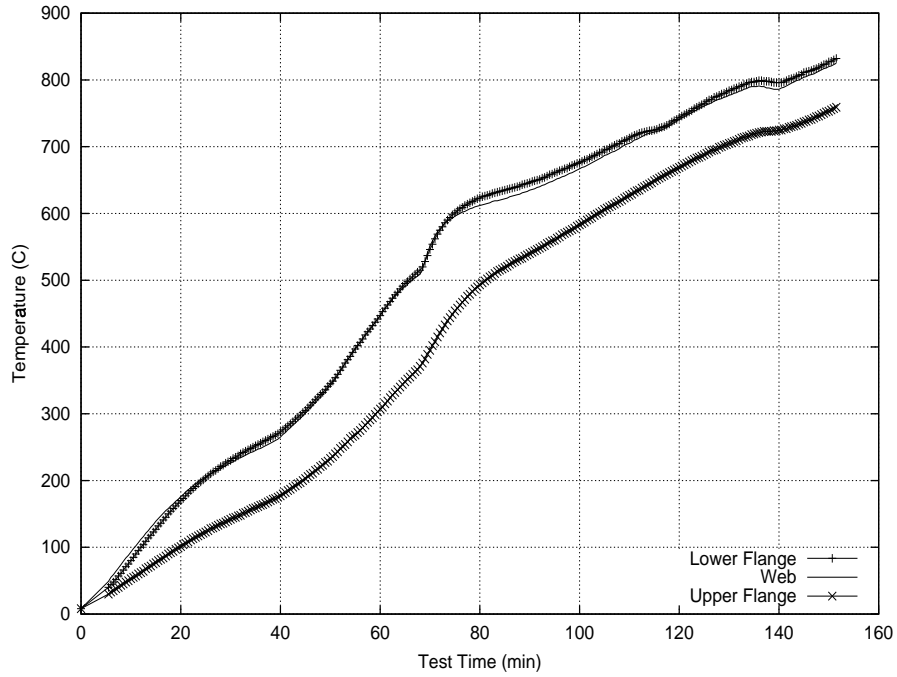


Figure 8: Experimental values of the beam temperature at three locations through its depth at typical section.

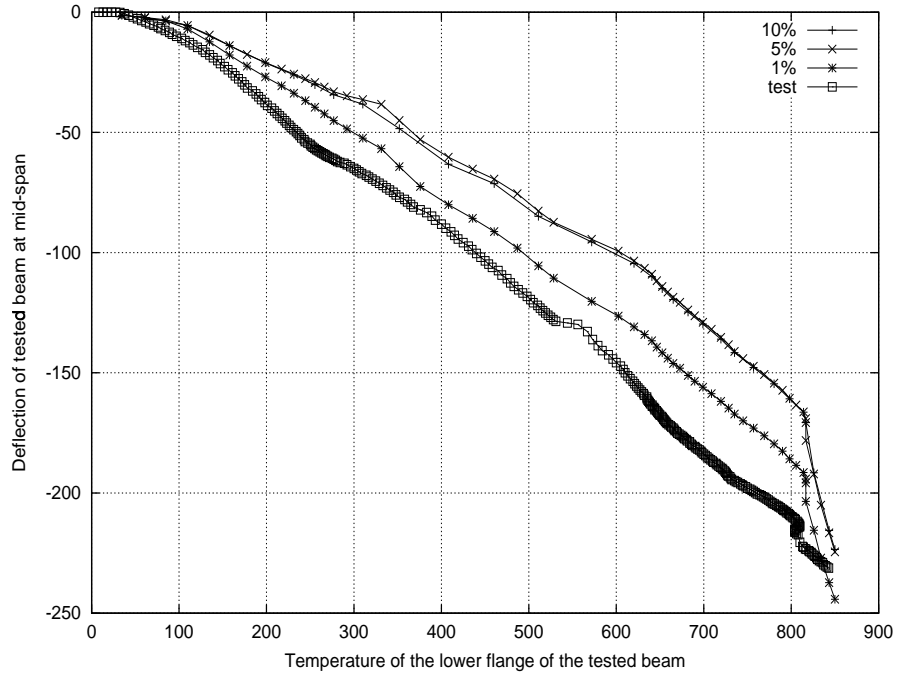


Figure 9: The effect of varying the concrete tensile strength on the mid-span deflection of test 1.

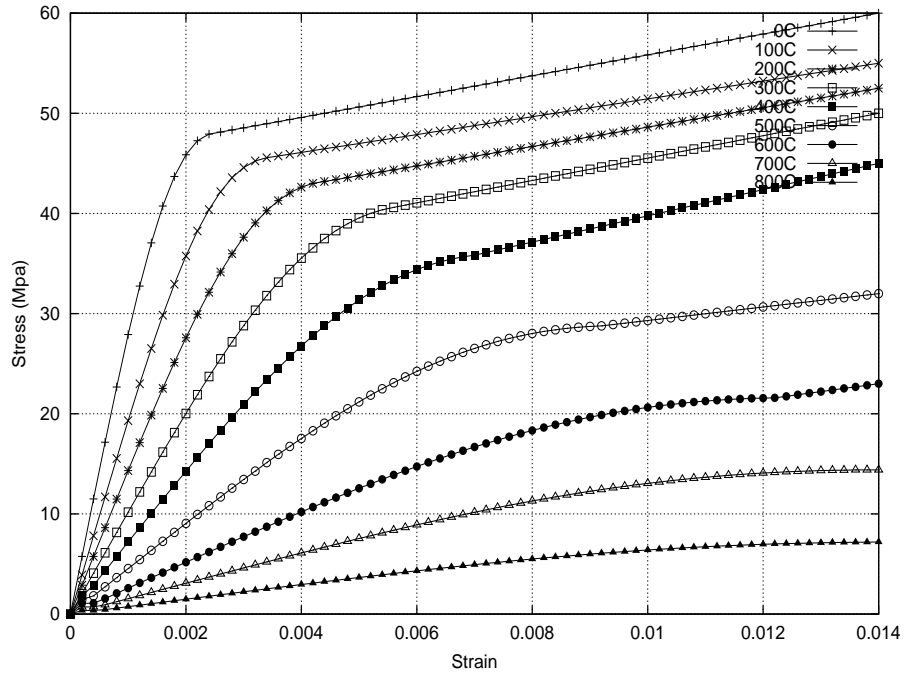


Figure 10: The concrete material behaviour used in FEA1 during the analysis of test 1

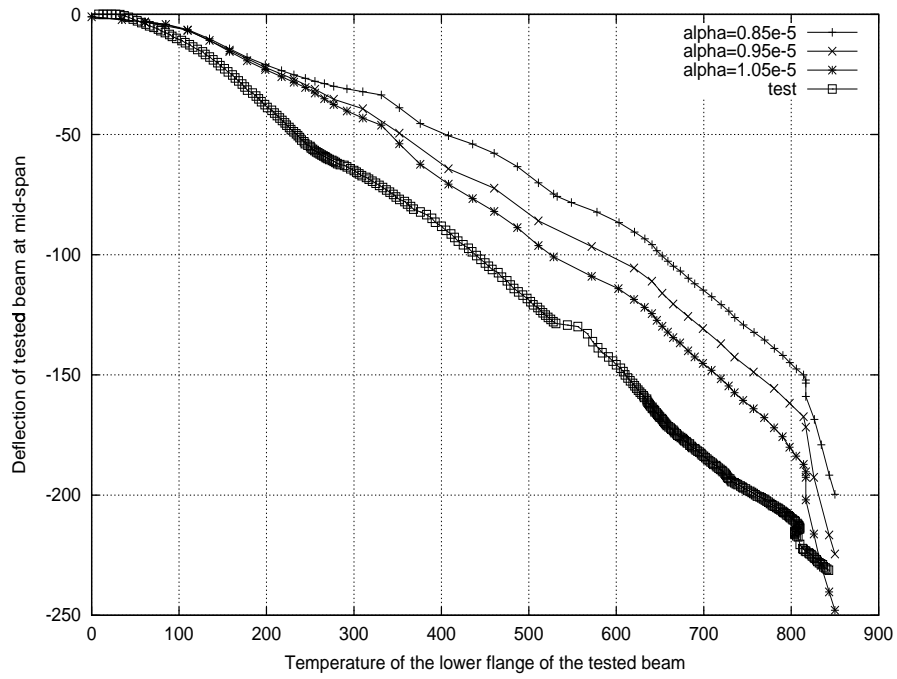


Figure 11: The effect of varying the coefficient of thermal expansion on the mid-span deflection of test 1.

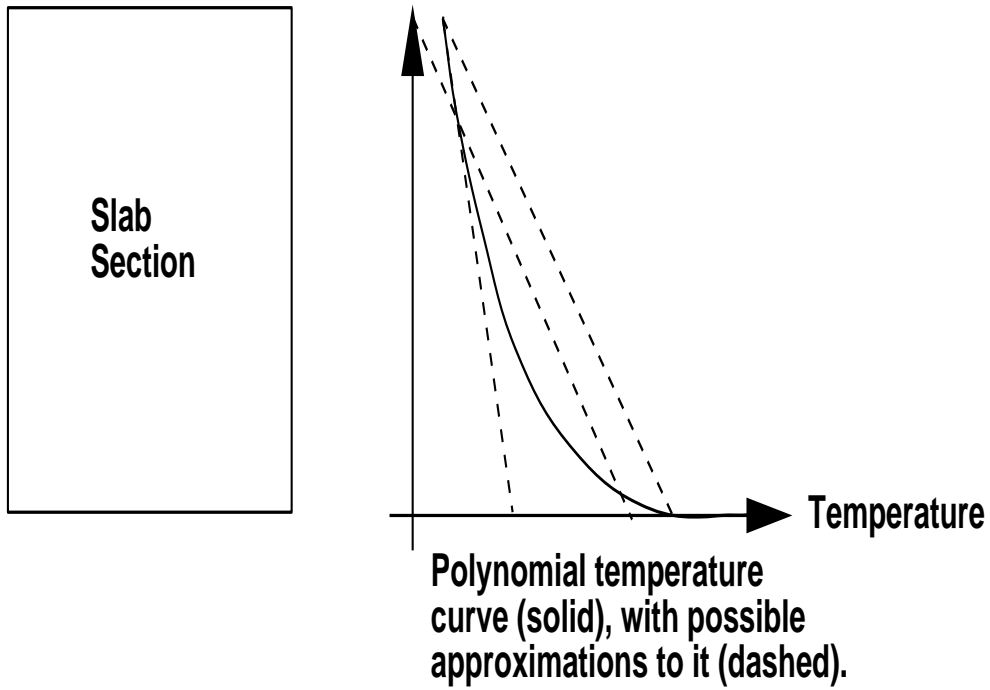


Figure 12: Possible linear approximations of a non-linear gradient.

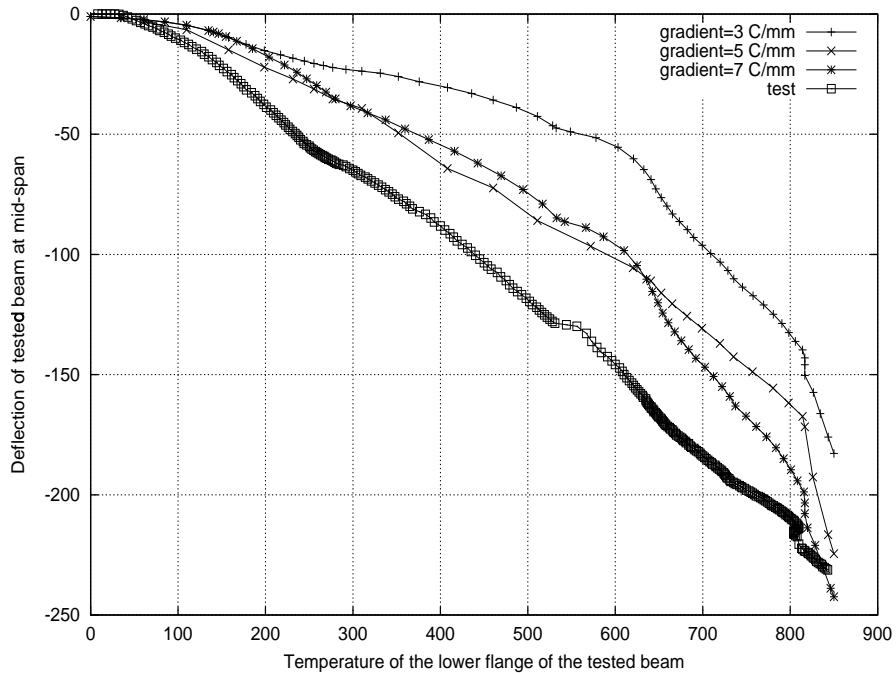


Figure 13: The effect of varying the final thermal gradient on the mid-span deflection of test 1.

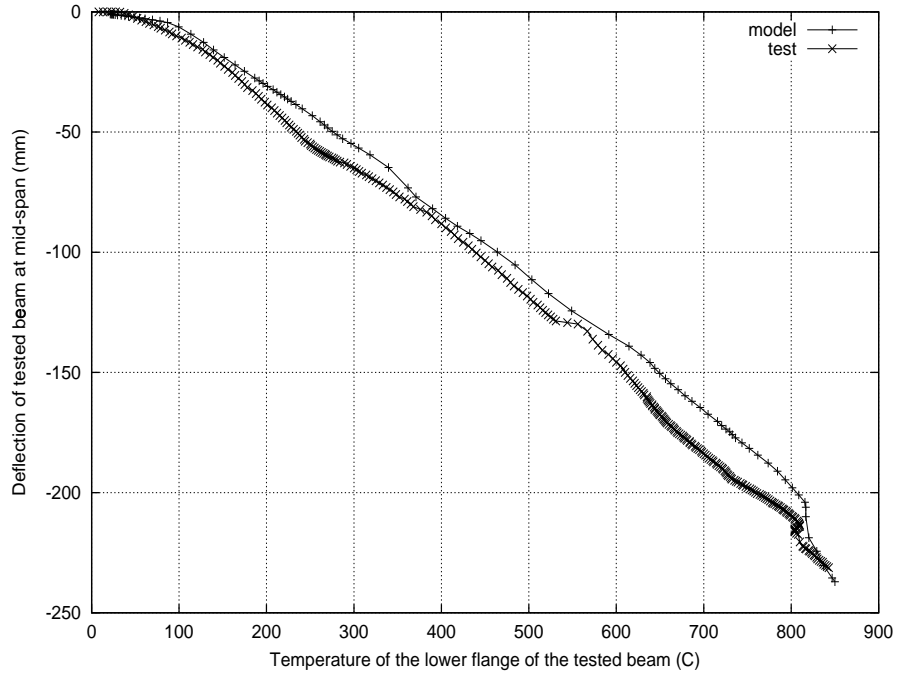


Figure 14: Deflection against beam lower flange temperature for the FEAST model of test 1.

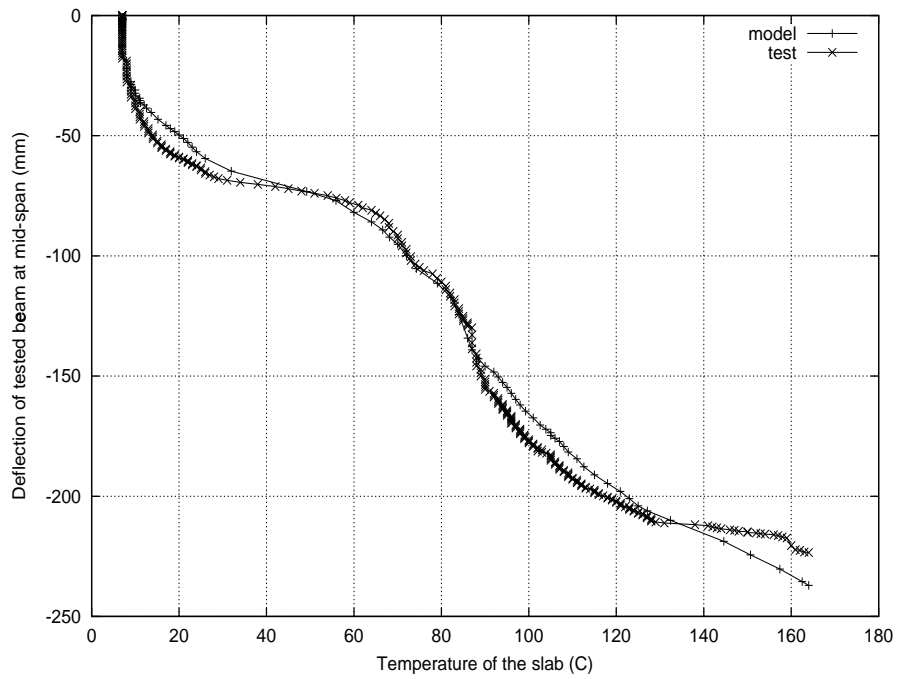


Figure 15: Deflection against slab reference surface temperature for the FEAST model of test 1.

A ABAQUS input for FEAST model of test 1

```
*HEADING
Input file for test1 using FEAST
*****
**                               NODE GENERATION                               **
*****
**
*NODE,INPUT=./INPUTDAT/Column1.res, NSET=COLUMNN
*NODE,INPUT=./INPUTDAT/Pbeam1.res,  NSET=PBEAMN
*NODE,INPUT=./INPUTDAT/BKSbeam1.res, NSET=BKSBEAMN
*NODE,INPUT=./INPUTDAT/FRSbeam1.res, NSET=FRSBEAMN
*NODE,INPUT=./INPUTDAT/LSbeam1.res,  NSET=LSBEAMN
*NODE,INPUT=./INPUTDAT/Web1.res,     NSET=RSBEAMN
*NODE,INPUT=./INPUTDAT/Slabs1.res,   NSET=SLAB1
**
*****
**                               ELEMENT GENERATION AND DEFINITION           **
*****
**
*ELEMENT,INPUT=./INPUTDAT/Column2.res,ELSET=COLUMN2,TYPE=B31
*ELEMENT,INPUT=./INPUTDAT/Pbeam2.res,ELSET=PBEAME,TYPE=B31
*ELEMENT,INPUT=./INPUTDAT/BKSbeam2.res,ELSET=BKSBEAME,TYPE=B31
*ELEMENT,INPUT=./INPUTDAT/FRSbeam2.res,ELSET=FRSBEAME,TYPE=B31
*ELEMENT,INPUT=./INPUTDAT/LSbeam2.res,ELSET=LSBEAME,TYPE=B31
*ELEMENT,INPUT=./INPUTDAT/Slabs2.res, ELSET=SLAB2,TYPE=S8R
**
*****
**
**   THE JOIST USING ONE BEAM
**
*ELEMENT,TYPE=B31
601,714,715
*ELGEN,ELSET=RSBEAME
601,30,1,1
**
*****
**
**   DEFINITION OF SECTIONS FOR BEAMS AND SHELL ELEMENTS                       **
*****
**
*ELSET,ELSET=COOLS2,GENERATE
10571,10574,1
10541,10544,1
10511,10514,1
10481,10484,1
10451,10454,1
10421,10424,1
10391,10394,1
10361,10364,1
10331,10334,1
10301,10304,1
*ELSET,ELSET=HOTS2,GENERATE
10575,10599
```

```

10545,10569
10515,10539
10485,10509
10455,10479
10425,10449
10395,10419
10365,10389
10335,10359
10305,10329
*SHELL GENERAL SECTION,ELSET=SLAB2,USER,PROPERTIES=3
100
0.95e-5,5,850
*HOURGLASS STIFFNESS
5.17500E+15,, 3.88125E+15
*TRANSVERSE SHEAR STIFFNESS
2.59e8,2.59e8,0
*SHELL GENERAL SECTION,ELSET=COOLS2,USER,PROPERTIES=3
100
0.95e-5,5,850
*HOURGLASS STIFFNESS
5.17500E+15,, 3.88125E+15
*TRANSVERSE SHEAR STIFFNESS
2.59e8,2.59e8,0
*SHELL GENERAL SECTION,ELSET=HOTS2,USER,PROPERTIES=3
100
0.95e-5,5,850
*HOURGLASS STIFFNESS
5.17500E+15,, 3.88125E+15
*TRANSVERSE SHEAR STIFFNESS
2.59e8,2.59e8,0
*USER SUBROUTINES,INPUT=../../ugens_store/NEW/muxdbout2.f
*USER SUBROUTINES,INPUT=../../ugens_store/NEW/mugensout2.f
*SHELL SECTION,ELSET=BFLANGEE,MATERIAL=STEEL
10.2,5
*SHELL SECTION,ELSET=TFLANGEE,MATERIAL=STEEL
10.2,5
*SHELL SECTION,ELSET=WEBE,MATERIAL=STEEL
6.1,5
*BEAM SECTION,ELSET=COLUMNNE,SECTION=I,MATERIAL=STEEL,POISSON=0
130.1, 260.2, 255.9, 255.9, 17.3, 17.3, 10.6
1,0,0
*BEAM SECTION,ELSET=LSBEAME,SECTION=I,MATERIAL=STEEL,POISSON=0
151.9,303.8,165.1,165.1,10.2,10.2,6.1
0,0,-1
*BEAM SECTION,ELSET=BKSBEAME,SECTION=I,MATERIAL=STEEL,POISSON=0
151.9,303.8,165.1,165.1,10.2,10.2,6.1
0,0,1
*BEAM SECTION,ELSET=FRSBEAME,SECTION=I,MATERIAL=STEEL,POISSON=0
151.9,303.8,165.1,165.1,10.2,10.2,6.1
0,0,1
*BEAM SECTION,ELSET=PBEAME,SECTION=I,MATERIAL=STEEL,POISSON=0
301,602,227.6,227.6,14.8,14.8,10.6
-1,0,0
*BEAM SECTION,ELSET=RSBEAME,SECTION=I,MATERIAL=STEEL,POISSON=0,TEMP=VALUES

```



```

151.9,303.8,165.1,165.1,10.2,10.2,6.1
0,0,1
*BEAM SECTION,ELSET=CONNECT,SECTION=CIRC,MATERIAL=STEEL,POISSON=0
9.5
*****
**DEFINING NODE SETS ON THE SLAB
*****
*NSET,NSET=SLABLB,UNSORTED
10000,10122,10244,10366,10488,10732,10854,10976,
11098,11220,11342,11464,11586,11708
*NSET,NSET=SLABLBI,UNSORTED
10061,10183,10305,10427,10549,10671,10793,10915,
11037,11159,11281,11403,11525,11647
*NSET,NSET=SLABLF,UNSORTED
13660,13538,13416,13294,13172,12928,12806,12684,
12562,12440,12318,12196,12074,11952
*NSET,NSET=SLABLFI,UNSORTED
12013,12135,12257,12379,12501,12623,12745,12867,
12989,13111,13233,13355,13477,13599
*NSET,NSET=SLABB,GENERATE
10000,10060,1
*NSET,NSET=SLABF,GENERATE
13660,13720,1
*NSET,NSET=SLABR,GENERATE
10060,13720,61
*NSET,NSET=SLABBSB,GENERATE
10610,10670,2
*NSET,NSET=SLABFSB,GENERATE
13050,13110,2
*NSET,NSET=SLABMSB,GENERATE
11830,11890,2
*NSET,NSET=SBEAMR,GENERATE
714,744,1
*NSET,NSET=PBEAM1,UNSORTED
2109,2110,2111,2112,2113,2115,2116,2117,2118,2119,2120,2121
,2122,2123
*NSET,NSET=PBEAM2,UNSORTED
2140,2139,2138,2137,2136,2134,2133,2132,2131,2130,2129,2128
2127,2126
**Grid on slab takes form
**
** D1 C1 B1
** D2 C2 B2
** D3 C3 B3 (over the beam's Centre Line, D = cold, C = Warm, B = Hot)
** D4 C4 B4
** D5 C5 B5
**
*NSET,GENERATE,NSET=HOTS
12442,12500,1
12381,12439,2
12320,12378,1
12259,12317,2
12198,12256,1
12137,12195,2

```

```

12076,12134,1
12015,12073,2
11954,12012,1
11893,11951,2
11832,11890,1
11771,11829,2
11710,11768,1
11649,11707,2
11588,11646,1
11527,11585,2
11466,11524,1
11405,11463,2
11344,11402,1
11283,11341,2
11222,11280,1
*NSET,GENERATE,NSET=COOLS
11222,12442,61
11223,12443,122
11224,12444,61
11225,12445,122
11226,12446,61
11227,12447,122
11228,12448,61
11229,12449,122
11230,12450,61
*****
**THESE NODES ARE USED TO DEFINE THE TEMP IN THE BEAM
*****
*NSET,NSET=HOTB,GENERATE
721,744,1
*NSET,NSET=COLDB
714
*NSET,NSET=COOLB,GENERATE
715,720,1
*****
** THESE SET OF NODE ARE USED TO DEFINE THE BOUNDARY CONDITION **
**           (FIXED BOUNDARY DEFINITIONS)           **
*****
*NSET,NSET=COLBASE
2234
*NSET,NSET=COLMID
2259
*NSET,NSET=COLMIDW
2264
*NSET,NSET=COLTOP
2294
*NSET,NSET=LSBEAML
2171
*NSET,NSET=LSBEAMR
2141
*NSET,NSET=BKSBEAML
2172
*NSET,NSET=BKSBEAMR
2202

```

```

*NSET,NSET=FRSBEAML
2203
*NSET,NSET=FRSBEAMR
2233
*NSET,NSET=PBEAMBK
2109
*NSET,NSET=PBEAMBKS
2114
*NSET,NSET=PBEAMBKC
2124
*NSET,NSET=PBEAMFRC
2125
*NSET,NSET=PBEAMFRS
2135
*NSET,NSET=PBEAMFR
2140
*NSET,NSET=WEBENDR
744
*NSET,NSET=WEBENDL
714
*****
** THESE SET OF NODE ARE USED TO DEFINE THE BOUNDARY CONDITION **
** (TIED BOUNDARY DEFINITIONS) **
*****
*NSET,NSET=LSBEAM2,GENERATE
2141,2171,2
*NSET,NSET=BKSBEAM2,GENERATE
2172,2202,2
*NSET,NSET=FRSBEAM2,GENERATE
2203,2233,2
*NSET,NSET=CWEB,GENERATE
714,744,2
*NSET,NSET=BWEBL,GENERATE
559,869,31
*NSET,NSET=COLFACER,GENERATE
2259,2269,1
*****
** END OF FILE FOR THE MESH GENERATION **
*****
** DEFINITION OF STEEL CHARACTERISTICS UNDER TEMPERATURE EFFECT **
** ( MATERIAL DEFINITION (FROM BS) ) **
*****
*MATERIAL, NAME=STEEL
*ELASTIC
210000.00,0.3, 20.0
210000.00,0.3, 100.0
210000.00,0.3, 200.0
210000.00,0.3, 300.0
210000.00,0.3, 400.0
163800.00,0.3, 500.0
98700.00,0.3, 600.0
48300.00,0.3, 700.0
23100.00,0.3, 800.0

```

```

12600.00,0.3, 900.0
8400.00,0.3, 1000.0
4200.00,0.3, 1100.0
*PLASTIC
300.4286 , 0.0000 , 20.0
301.8214 , 0.0046 , 20.0
303.2143 , 0.0092 , 20.0
304.6071 , 0.0138 , 20.0
306.0000 , 0.0184 , 20.0
390.0000 , 0.0378 , 20.0
431.2500 , 0.1385 , 20.0
** 0.0450 , 0.1811 , 20.0
300.4286 , 0.0000 , 100.0
301.8214 , 0.0046 , 100.0
303.2143 , 0.0092 , 100.0
304.6071 , 0.0138 , 100.0
306.0000 , 0.0184 , 100.0
390.0000 , 0.0378 , 100.0
431.2500 , 0.1385 , 100.0
** 0.0450 , 0.1811 , 100.0
242.4101 , 0.0000 , 200.0
281.7419 , 0.0047 , 200.0
295.2222 , 0.0093 , 200.0
302.6983 , 0.0139 , 200.0
306.0000 , 0.0185 , 200.0
389.9446 , 0.0378 , 200.0
431.1946 , 0.1385 , 200.0
** 0.0450 , 0.1811 , 200.0
184.1013 , 0.0000 , 300.0
260.7255 , 0.0047 , 300.0
286.8511 , 0.0094 , 300.0
300.6972 , 0.0141 , 300.0
306.0000 , 0.0187 , 300.0
390.0000 , 0.0382 , 300.0
431.2500 , 0.1388 , 300.0
** 0.0450 , 0.1814 , 300.0
126.1080 , 0.0000 , 400.0
238.6160 , 0.0048 , 400.0
278.0298 , 0.0095 , 400.0
298.5857 , 0.0143 , 400.0
306.0713 , 0.0190 , 400.0
390.0891 , 0.0384 , 400.0
431.3391 , 0.1390 , 400.0
** 0.0450 , 0.1816 , 400.0
** The next values are modified by AMS on 1/10/98
** 108.0926 , 0.0000 , 500.0
80.0926 , 0.0000 , 500.0
190.0915 , 0.0048 , 500.0
218.4475 , 0.0095 , 500.0
233.2746 , 0.0143 , 500.0
238.6800 , 0.0190 , 500.0
243.3600 , 0.0384 , 500.0
269.1000 , 0.1390 , 500.0
** 0.0281 , 0.1816 , 500.0

```

** The next values are modified by AMS on 1/10/98

** 54.0448 , 0.0000 , 600.0

41.0448 , 0.0000 , 600.0

109.9982 , 0.0048 , 600.0

129.8143 , 0.0095 , 600.0

140.1297 , 0.0143 , 600.0

143.8200 , 0.0190 , 600.0

146.6400 , 0.0384 , 600.0

162.1500 , 0.1390 , 600.0

** 0.0169 , 0.1816 , 600.0

22.5185 , 0.0000 , 700.0

52.0548 , 0.0048 , 700.0

62.8152 , 0.0095 , 700.0

68.4043 , 0.0143 , 700.0

70.3800 , 0.0190 , 700.0

71.7600 , 0.0384 , 700.0

79.3500 , 0.1390 , 700.0

** 0.0083 , 0.1816 , 700.0

15.0119 , 0.0000 , 800.0

26.7412 , 0.0048 , 800.0

30.7799 , 0.0096 , 800.0

32.8910 , 0.0143 , 800.0

33.6600 , 0.0190 , 800.0

34.3200 , 0.0385 , 800.0

37.9500 , 0.1391 , 800.0

** 0.0040 , 0.1817 , 800.0

11.2589 , 0.0000 , 900.0

15.7446 , 0.0048 , 900.0

17.2502 , 0.0096 , 900.0

18.0504 , 0.0143 , 900.0

18.3600 , 0.0190 , 900.0

18.7200 , 0.0385 , 900.0

20.7000 , 0.1391 , 900.0

** 0.0022 , 0.1817 , 900.0

7.5060 , 0.0000 ,1000.0

10.4964 , 0.0048 ,1000.0

11.5002 , 0.0096 ,1000.0

12.0336 , 0.0143 ,1000.0

12.2400 , 0.0190 ,1000.0

12.4800 , 0.0385 ,1000.0

13.8000 , 0.1391 ,1000.0

** 0.0014 , 0.1817 ,1000.0

3.7530 , 0.0000 ,1100.0

5.2482 , 0.0048 ,1100.0

5.7501 , 0.0096 ,1100.0

6.0168 , 0.0143 ,1100.0

6.1200 , 0.0190 ,1100.0

6.2400 , 0.0385 ,1100.0

6.9000 , 0.1391 ,1100.0

** 0.0007 , 0.1817 ,1100.0

*EXPANSION

1.23E-5,20.

1.23E-5,50.

1.25E-5,100.

1.27E-5,150.
 1.29E-5,200.
 1.31E-5,250.
 1.33E-5,300.
 1.35E-5,350.
 1.37E-5,400.
 1.39E-5,450.
 1.41E-5,500.
 1.43E-5,550.
 1.45E-5,600.
 1.47E-5,650.
 1.49E-5,700.
 1.51E-5,750.
 1.41E-5,800.
 1.33E-5,850.
 1.34E-5,900.
 1.38E-5,950.
 1.41E-5,1000.
 1.44E-5,1050.
 1.46E-5,1100.
 1.49E-5,1150.
 1.51E-5,1200.

 ** END OF FILE FOR STEEL CHARACTERISTICS **

 ** GENERATION OF BOUNDARY CONDITIONS **
 ** 1) STRUCTURAL CONDITIONS, 2) THERMAL CONDITIONS *****

**
 *INITIAL CONDITIONS,TYPE=TEMPERATURE
 COLUMN,0
 PBEAMN,0
 BKSBEAMN,0
 FRSBEAMN,0
 LSBEAMN,0
 RBEAMN,0
 SLAB1,0

 ** CONNECTION OF VARIOUS ELEMENT SETS (MPCS) **

**
 **TIE CENTRE LINE OF SLAB TO CENTRE LINE OF TOP FLANGE
 ** 4 SECONDARY BEAMS TO PRIMARY BEAM
 *MPC
 BEAM,BKSBEAML,PBEAMBKS
 BEAM,FRSBEAML,PBEAMFRS
 **

** RIGHT SECONDARY BEAM AND PRIMARY BEAMS TO COLUM
 **
 *MPC
 BEAM,PBEAMBKC,COLMID
 BEAM,PBEAMFRC,COLMID
 BEAM,LSBEAMR,COLMIDW

```

BEAM,WEBENDL,COLMIDW
**TYING THE SLAB TO THE BEAMS
**
*MPC
**SLAB TO PRIMARY BEAMS
BEAM,SLALB,PBEAM1
BEAM,SLALF,PBEAM2
**BEAM,SLALBI,PBEAM1
**BEAM,SLALFI,PBEAM2
**SLAB TO SECONDARY BEAMS
BEAM,SLABFSB,FRSBEAMN
BEAM,SLABBSB,BKSBEAMN
BEAM,SLABMSB,SBEAMR
*****
**                               FIXED BOUNDARY CONDITIONS                               **
*****
*BOUNDARY
PBEAMFRS,1,
PBEAMFRS,5,6
PBEAMBKS,1,
PBEAMBKS,5,6
**      column - fixed at bottom vertical deflection at top
COLTOP,1,
COLTOP,3,6
COLBASE,1,6
** TRYING WITH A FIXED COLUMN
COLMIDW,5
**                               primary beam
PBEAMFR,1,
PBEAMFR,3,6
PBEAMBK,1,
PBEAMBK,3,6
PBEAMN,1
PBEAMN,6
**
** FIXING THE ENDS OF THE P.BEAMS AND THE LEFT S.BEAM
**                               secondary beam (left of column)
**
LSBEAML,1,
LSBEAML,3,6
**
**                               secondary beam (right of column)
**
WEBENDR,1
WEBENDR,5,6
BKSBEAMR,1
BKSBEAMR,5,6
FRSBEAMR,1
FRSBEAMR,5,6
**
**      slab boundary conditions
**
SLABB,1
SLABB,3,5

```

```

SLABF, 1
SLABF, 3, 5
SLABR, 1
SLABR, 5, 6
*****
*****          END OF BOUNDARY & INITIAL CONDITIONS          **
*****
*RESTART,WRITE,FREQUENCY=1
*****
**              I)  STATIC LOAD              **
*****
*STEP,AMPLITUDE=RAMP,INC=20,NLGEOM
*STATIC
1,, ,
*DLOAD,OP=NEW
LSBEAME,PY,-16.44
SLAB2,P,0.00548
*TEMPERATURE,OP=NEW
*NODE FILE,FREQ=5
U
RF
*EL FILE,FREQ=5
1
S,E
*MONITOR,NODE=744,DOF=2
*END STEP
*****
**              2)  TEMPERATURE PROFILE              **
*****
*STEP,AMPLITUDE=RAMP,INC=400,NLGEOM
*STATIC
15,850,1E-4,15
*AMPLITUDE,NAME=SLABTEMP,INPUT=./INPUTDAT/slabtemp3,VALUE=RELATIVE
*AMPLITUDE,NAME=BEAMTEMP,INPUT=./INPUTDAT/beamtemp,VALUE=RELATIVE
*TEMPERATURE,AMPLITUDE=SLABTEMP
HOTS,164
COOLS,164
*TEMPERATURE,AMPLITUDE=BEAMTEMP
HOTB,850,850,800,750,750
COOLB,850,850,800,750,750
COLDB,30,30,30,30,30
*END STEP

```


B FEAI input file for the slab parallel to the ribs

```
33      300
0       300      50
-0.01      0.01      0.0005
-0.00049   0.0005   0.00001
70
125     90      1      1
115     690    1      1
105     690    1      1
95      690    1      1
85      690    1      1
75      690    1      1
65      690    1      1
55      345    1      1
125    1620    1      2
115    1620    1      2
105    1620    1      2
95     1620    1      2
85     1620    1      2
75     1620    1      2
65     1620    1      2
55     810     1      2
45     1600    1      2
35     1525    1      2
25     1450    1      2
15     1400    1      2
5      1360    1      2
125     690    1      1
115     690    1      1
105     690    1      1
95      690    1      1
85      690    1      1
75      690    1      1
65      690    1      1
55      345    1      1
65      200    3      2
27.5   60.8   2      2
0      122.4  2      2
55     100    2      2
```

C FEAI input file for the slab perpendicular to the ribs

```
8 300
00 300 50
-0.01 0.01 0.0005
-0.00049 0.0005 0.00001
10
65 3000 1 1
55 3000 1 1
45 3000 1 1
35 3000 1 1
25 3000 1 1
15 3000 1 1
05 3000 1 1
15 200 3 1
```